# Interaction between Dicarboxylic Acid and Sulfuric Acid-Base Clusters

Yun Lin,[1] Yuemeng Ji,[1,2,*] Yixin Li,[1] Jeremiah Secrest,[1] Wen Xu,[3] Fei Xu,[4] Yuan Wang,[5] Taicheng An,[2] and Renyi Zhang[1,*]

[1]Department of Atmospheric Sciences and Department of Chemistry, Texas A&M University, College Station, TX 77843, USA

[2]Institute of Environmental Health and Pollution Control, Guangdong University of Technology, Guangzhou 510006, China

[3]Aerodyne Research Inc, Billerica, MA 01821, USA

[4]School of Environmental Science and Engineering, Shandong University, Jinan 250100, China

[5]Division of Geological and Planetary Sciences, California Institute of Technology, Pasadena, CA, 91125, USA

* Corresponding authors: Renyi Zhang, renyi-zhang@tamu.edu; Yuemeng Ji, jiym99@163.com

**ABSTRACT.** Dicarboxylic acids likely participate in the formation of pre-nucleation clusters to facilitate new particle formation in the atmosphere, but the detailed mechanism leading to the formation of multi-component critical nucleus involving organic acids, sulfuric acid (SA), base species, and water remains unclear. In this study, theoretical calculations are performed to elucidate the interactions between succinic acid (SUA) and clusters consisting of SA-ammonia (AM)/dimethylamine (DMA) in the presence of hydration of up to six water molecules. Formation of the hydrated SUA•SA•base clusters is energetically favorable, triggering proton transfer from SA to the base molecule to form new covalent bonds or strengthening the pre-existing covalent bonds. The presence of SUA promotes hydration of the SA•AM and SA•AM•DMA clusters but dehydration of the SA•DMA clusters. At equilibrium, SUA competes with the second SA molecule for addition to the SA•base clusters at atmospherically relevant concentrations. The clusters containing both the base and organic acid are capable of further binding with acid molecules to promote subsequent growth. Our results indicate that the multi-component nucleation involving organic acids, sulfuric acid, and base species promotes new particle formation in the atmosphere, particularly under polluted conditions.

## 1. INTRODUCTION

Atmospheric aerosols are important to several issues, including climate, visibility and human health (IPCC, 2013; Zhang et al., 2015). In particular, aerosols influence the Earth energy budget directly by absorbing/scattering incoming solar radiation and indirectly by acting as cloud condensation nuclei (CCN)/ice nuclei (IN), which impact the lifetime, coverage, precipitation efficiency, and albedo of clouds (Andreae et al., 2004; Fan et al., 2007; Li et al., 2008). Currently, the indirect radiative forcing of aerosols represents the largest uncertainty in climate predictions (IPCC, 2013). New particle formation (NPF) has been observed under diverse environmental conditions (Kulmala and Kerminen, 2008; Zhang et al., 2012; Guo et al., 2014; Bianchi et al., 2016; Wang et al., 2016) and contributes up to half of the CCN population in the troposphere (Merikanto et al., 2009; Yue et al., 2011). NPF involves two distinct steps, i.e., nucleation to form a critical nucleus and subsequent growth of newly formed nanoparticles to a larger size (> 3 nm). Currently, the identities and the roles of chemical species involved in NPF are not fully understood at the molecular level, hindering the development of physically-based parameterization to include NPF in atmospheric models (Zhang et al. 2010; Cai and Jiang, 2017). Sulfuric acid (SA) is believed to be the most common atmospheric nucleation species, and ammonia (AM)/amines further stabilize the hydrated sulfuric acid clusters and enhance the nucleation (Kuang et al, 2010; Yue et al., 2010; Erupe et al., 2011; Yu et al., 2012; Qiu et al., 2013; Wang et al., 2018; Yao et al., 2018). However, neither the sulfuric acid-water binary nucleation nor ammonia/amine-containing ternary nucleation sufficiently explains the measured NPF rates in the lower troposphere (Xu et al., 2010a; Zhang et al. 2012), suggesting the role of other chemical species, such as organic acids, in NPF (Zhang et al., 2004; McGraw and Zhang, 2008).

The role of organic species in assisting aerosol nucleation and growth has been demonstrated by both experimental and theoretical studies (Zhang et al., 2009; Zhao et al., 2009; Wang et al., 2010; Xu et al., 2010b; Xu et al., 2012; Elm et al., 2014; Weber et al., 2014; Xu et al., 2014; Zhu et al., 2014; Tröstl et al., 2016). However, the interactions between organic acids and the other nucleation precursors are still elusive, due to the large variability in the physicochemical nature of organic acids, e.g., the wide range of volatility and functionality (Zhang et al., 2012; Riccobono et al., 2014). In addition, most of the previous theoretical studies focus on the enhancement effects of organic acids on the SA-$H_2O$ binary nucleation or the role of organic acids in clustering basic species such as ammonia or amines with hydration (Zhao et al., 2009; Xu et al., 2010; Xu et al. 2013; Elm et al., 2014; Weber et al., 2014; Zhu et al., 2014). Several recent studies have been conducted on the underlying mechanisms of organic acids in large pre-nucleation clusters (e.g. ammonia/amine-containing ternary nucleation) (Xu et al., 2010; Xu et al., 2012; Elm et al., 2016a; Zhang et al., 2017), but most of these studies treated the clusters without the consideration of hydration. Because of the ubiquitous presence of water (W) in the atmosphere and its much higher abundance than other nucleation precursors, the hydration effect on aerosol nucleation is significant (Loukonen et al., 2010; Xu and Zhang, 2013; Henschel et al., 2014; Zhu et al., 2014; Henschel et al., 2016).

Atmospheric measurements have shown that the presence of dicarboxylic acids, including succinic acid (SUA), is prevalent in ambient particles (Kawamura and Kaplan, 1987; Decesari et al., 2000; Legrand et al., 2005; Hsieh et al. 2007; Blower et al., 2013). The effect of dicarboxylic acids on aerosol nucleation involving SA or base molecules has been recognized in theoretical studies. Xu and Zhang (2012) showed that dicarboxylic acids promote aerosol nucleation with other nucleating precursors in two directions via hydrogen bonding to the two carboxylic groups

on dicarboxylic acids, which is distinct from monocarboxylic acids. Elm et al. (2014) indicated that clustering of a single pinic acid with SA molecules leads to closed structures because of no available sites for additional hydrogen bonding. In addition, Elm et al. (2017) suggested that more than two carboxylic acid groups are required for a given organic oxidation product to efficiently stabilize sulfuric-acid contained clusters. The interaction between SUA and dimethylamine (DMA) is strengthened by hydration via forming aminium carboxylate ion pairs (Xu and Zhang, 2013), while hydration of oxalic acid-AM cluster is somewhat unfavorable under atmospheric conditions (Weber et al., 2014). Clearly, the interactions of dicarboxylic acids with other nucleation precursors depend on the type of dicarboxylic acids and the number of the molecules involved in clustering. Presently, theoretical studies on the effect of dicarboxylic acids on nucleation from multi-component systems are lacking (Xu et al., 2010; Xu and Zhang, 2013). In particular, the role of organic acids as well as their participation in stabilizing larger pre-nucleation clusters of the SA-ammonia/amine systems needs to be evaluated with the presence of hydration in order to better understand NPF.

In this study, we performed theoretical calculations to evaluate the effect of SUA on hydrated SA•base clusters. Two base species, ammonia and dimethylamine (DMA), were considered. The Basin Paving Monte Carlo (BPMC) method was employed to sample stable cluster conformers, and quantum calculations were performed to predict the thermochemical properties of the multi-component clusters. Geometric and Topological analyses were carried out to investigate the structures and binding between SUA and SA•base clusters in the presence of hydration. The implications of the interaction of SUA with hydrated SA-base clusters for atmospheric NPF are discussed.

## 2. COMPUTATIONAL METHODS

The methodology of the BPMC conformational sampling combined with quantum calculations using density functional theory (DFT) was employed to assess the role of SUA in clustering of SA with base compounds in the presence of water (Xu and Zhang, 2013). Briefly, the local energy minima in BPMC simulations was searched by using Amber11 package, and the Basin Hopping Monte Carlo (BHMC) approach was employed to increase the Monte Carlo transition probability, which allows the clustering system to escape from the traps of local energy minimum. We employed the Generalized Amber Force Field (GAFF) for AM, DMA and SUA following Wang et al. (2004; 2006). The force field parameters from Loukonen et al. (2010) were adapted for SUA and bisulfate ion. Hydration of the clustering system was evaluated by employing the TIP3P model. The geometric optimization and frequency calculations of the BPMC sampled cluster complexes were further performed at PW91PW91 level of theory with the basis set 6-311++G(2d, 2p) using Gaussian 09 software package (Frisch et al., 2009). Thermodynamic quantities, such as the electronic energy ($\Delta E$ with ZPE), enthalpy ($\Delta H$), and Gibbs free energies ($\Delta G$), were obtained on the basis of unscaled density functional frequencies at temperature of 298.15 K and pressure of 1 atm. Several basic cluster systems were also examined at the M06-2X/6-311++G(3df,3pd) level of theory, which has been suggested to be more reliable in predicting binary/ternary cluster formation (Elm and Mikkelsen, 2012; Leverentz et al., 2013; Zhang et al., 2017). Comparisons of the free energies with the two different DFT levels of theories between this study and previous available theoretical and experimental studies are presented in Table 1. The energies derived at the PW91PW91/6-311++G(2d, 2p) are consistent with those of the M06-2X/6-311++G(3df,3pd) method, and the differences between our calculations and previous studies are

119 within 1.6 kcal $mol^{-1}$. The thermochemical quantities calculated at the PW91PW91/6-311++G(2d,
120 2p) level of theory for the most stable cluster configurations are summarized in Table 2.
121 Topological analysis on the SA•base clusters with hydration and SUA was performed by
122 employing the Multifunctional Wavefunction Analyzer (Multiwfn) 3.3.8 program (Lu and Chen,
123 2012). The topological characteristics at the bond critical points (BCPs) were calculated for
124 electron density (ρ), Laplacian of electron density (Δρ), and potential energy density (*V*). Since the
125 electron density is highly correlated to bonding strength (Lane et al., 2013), the potential energy
126 density is an indicator of hydrogen bond energies (Espinosa et al., 1998). The occurrence of proton
127 transfer in the clusters was determined using the localized orbital locator (LOL). A high LOL value
128 denotes greatly localized electrons and indicates the existence of a covalent bond (Lu et al., 2012).
129 The covalent bond is characterized by a negative Δρ, while a positive Δρ is associated with a
130 hydrogen bond. In addition, a newly formed covalent bond via proton transfer was quantitatively
131 examined in terms of the bond strength using the Laplacian bond order (LBO) as an indicator (Lu
132 et al., 2013). Both LOL and LBO were calculated with Multiwfn 3.3.8 program (Lu et al., 2012).
133 The extent, to which clusters are hydrated (or the hydrophilicity of the clusters), is affected
134 by humidity conditions in the atmosphere (Loukonenet al., 2010; Henschel et al., 2014; Henschel
135 et al., 2016). To examine the influence of SUA on cluster hydration under different humidity
136 conditions, the relative hydrate distributions over the number of water molecules contained in
137 clusters were calculated at different relative humidity (RH) levels. The distribution was calculated
138 according to Henschel et al. (2014), in which the Gibbs free energies of hydration obtained from
139 DFT calculations are converted to equilibrium constants for the formation of the respective hydrate
140 by

141 $$K = e^{\frac{-\Delta G^0}{RT}} \quad (1)$$

and the relative hydrate population $x_n$ of the hydrate containing $n$ water molecules is determined by

$$x_n = \left(\frac{p(\mathrm{H_2O})}{p^0}\right)^n x_0 e^{\frac{-\Delta G_n}{RT}} \quad (2)$$

where $p(\mathrm{H_2O})$ is the water partial pressure, $p^0$ is the pressure of water at 1 atm, $x_0$ is the population of the dry cluster for $\sum_0^6 x_n = 1$, $T$ is the standard temperature (298.15 K), and $R$ is the molar gas constant. $p(\mathrm{H_2O})$ is related to RH through

$$p(\mathrm{H_2O}) = p(\mathrm{H_2O})_{eq} \times RH \quad (3)$$

where $p(\mathrm{H_2O})_{eq}$ is the water saturation vapor pressure, which is a function of the temperature (Wexler, 1976). Note that only the Gibbs free energy for the lowest energy structure for each hydration was considered and the Boltzmann averaging effect over configurations on comparable clusters was negligible for the free energies of hydration (Erupe et al., 2011; Xu and Zhang, 2013; Tsona et al., 2015).

To assess the importance of uptake of SUA on the SA•base clusters under atmospheric conditions, the ratio in the concentrations SA•X•SUA to $(SA)_2$•X (X denotes either AM or DMA) is estimated under equilibrium conditions,

$$\mathrm{SA \cdot X + SUA = SA \cdot X \cdot SUA} \quad (4)$$

$$\mathrm{SA \cdot X + SA = (SA)_2 \cdot X} \quad (5)$$

and the equilibrium constants $K_1$ and $K_2$ for reactions (4) and (5) are expressed as

$$K_1 = \frac{[\mathrm{SA \cdot X \cdot SUA}]}{[\mathrm{SA \cdot X}][\mathrm{SUA}]} = e^{\frac{-\Delta G_1}{RT}} \quad (6)$$

$$K_2 = \frac{[(\mathrm{SA})_2 \cdot \mathrm{X}]}{[\mathrm{SA \cdot X}][\mathrm{SA}]} = e^{\frac{-\Delta G_2}{RT}} \quad (7)$$

The ratio between SA•X•SUA and $(SA)_2$•X concentrations is derived by dividing $K_1$ and $K_2$,

$$\frac{[SA \cdot X \cdot SUA]}{[(SA)_2 \cdot X]} = \frac{[SUA]}{[SA]} e^{\frac{-\Delta(\Delta G)}{RT}} \quad (8)$$

where $\Delta(\Delta G)$ is the difference in the Gibbs free energies between reactions (4) and (5) at 298 K. As listed in Table 3, the concentrations of sulfuric acid, ammonia, and dimethylamine in the atmosphere are typically in the range of $10^5 \sim 10^7$, $10^9 \sim 10^{11}$, $10^7 \sim 10^9$ molecules $cm^{-3}$ (Zhang et al., 2012), and the SUA concentration is in the range of $10^8 \sim 10^9$ molecules $cm^{-3}$ (Ho et al., 2007), resulting a SUA/SA ratio from 10 to $10^4$. In addition, the cluster concentration, [cluster], for addition of another monomer to the SA•base dimer with or without SUA is estimated from the atmospheric concentrations of the various precursors,

$$[cluster] = [SA] \times [X]\, e^{\left(\frac{-\Delta G}{RT}\right)} \qquad (9)$$

where *X* corresponds to AM, DMA, or SUA.

## 3. RESULTS AND DISCUSSION

### 3.1 STRUCTURES AND TOPOLOGY

The most stable structures (in terms of $\Delta G$ at $T$ = 298.15K and $p$ = 1 atm) of the hydrated SA•base clusters are shown in Figures 1-3. Addition of SUA to hydrated SA•base clusters alters the hydrogen-bonding and rearranges the cluster structure, affecting the free energy and stability for the cluster formation.[15] Proton transfer occurs with SUA addition to SA•base, leading to a conversion from the hydrogen bond to covalent bond within the cluster. Proton transfer is absent in the SA•AM cluster (Figure 1a), consistent with the previous studies (Kurtén et al., 2006; Loukonen et al., 2010; Henschel et al., 2014), while the occurrence of proton transfer with SUA addition (Figure 1b) is confirmed by the relocation of the LOL high value (Figure 4a). For the SA•AM cluster, a large value of LOL is adjacent to the SA molecule, indicating that electrons attained to the hydrogen atom (H1) on the S-O-H group are localized on the SA molecule side. In contrast, a large LOL region is located near the nitrogen atom (N1) on the AM molecule with the addition of SUA, suggesting that electrons are greatly localized on the AM side. Proton transfer

converts the N1-H1 hydrogen bonding to a covalent bond, leading to the formation of ammonium bisulfate with a value of 0.464 for LBO. The formation of the covalent bond is also confirmed by the negative sign of $\nabla\rho$ at BCP of N1-H1 bond (Table S1). The electron density (potential energy density) at BCP of the N1-H1 bond exhibits a significant increase (decrease), from 0.091 (-0.087) a.u. in the SA•AM cluster to 0.271 (-0.424) a.u. in the SA•AM•SUA cluster. The structures of SA•AM and SA•DMA hydrates with up to five water molecules in our calculations are consistent with those of Henschel et al. (2014). The interactions between SA and AM/DMA in the presence of hydration were previously studied (DePalma et al., 2012; Yu et al., 2012; Qiu et al., 2013; Xu and Zhang, 2013; Tsona et al., 2015), showing strong hydrogen bonding among SA, base compound, and water molecules. Another study on glycolic acid found that addition of one glycolic acid molecule to the SA•AM cluster does not result in proton transfer, unless a second glycolic acid molecule is added (Zhang et al., 2017). Clearly, SUA is more efficient than glycolic acid to stabilize the SA•AM clusters.

In contrast to the SA•AM cluster, proton transfer occurs for the SA•DMA cluster without water or SUA (Figures 2 and 4b), because of stronger basicity of DMA than AM (Anderson et al., 2008). Similarly, proton transfer occurs for the SA•AM•DMA cluster, leading to the formation of the aminium bisulfate ($HSO_4^-$) ion pair. Addition of SUA to SA•DMA•AM•$(W)_n$ results in additional proton transfer between the bisulfate ion and AM, leading to the formation of sulfate ions ($SO_4^{2-}$) (Figures 3 and 4c).

The dependence of the number of proton transfers on hydration is summarized in Table 4. For comparison, the results of hydration of SA clusters by Xu and Zhang (2013), who employed a similar method for the structure sampling and quantum calculations, are also included in this table. Both hydration and addition of SUA promote proton transfer in the SA•base clusters. Previous

studies identified facile proton transfer by hydration (Ding et al., 2003; Al Natsheh et al., 2004; Loukonen et al., 2010; Xu and Zhang, 2013), and the dependence of proton transfer on the hydration level was also indicated by Tsona et al. (2015). For the SA cluster, Xu and Zhang (2013) found that proton transfer in the hydrated SA clusters only occurs with more than two water molecules. In our study, proton transfer due to hydration occurs in the monohydrate of SA•AM. A second proton transfer also occurs due to hydration, for example, when SA•AM•DMA•$(W)_5$ clusters are hydrated with one more water molecule (Figures 1a and 3a). The formation of the covalent bond in the monohydrate of SA•AM and the sixth hydrate of SA•AM•DMA is confirmed by the LOL relocation (Figure S1). Loukonen et al. (2010) also found that proton transfer occurs in SA•AM for the hydrated cluster with two water molecules. Our results show that neither water molecules nor SUA induce the second proton transfer in SA•DMA clusters. In contrast, Loukonon et al. (2010) showed that the second proton transfer occurs when the SA•DMA cluster is hydrated with five water molecules. The difference in proton transfer with hydration between this study and Loukonen et al. is attributable to the different sampling methodology used to obtain the most stable conformers of the clusters. Note that the findings of Loukonen et al. are also in contrast to those by Henschel et al. (2014).

Table 5 summarizes the available LBO values for the covalent bonds in the SA•base clusters with hydration. The dependence of LBO on the hydration level varies with the clusters. For SA•AM without SUA, additional water molecules result in higher LBO of N1-H1 bonds, while for SA•DMA LBO of the N2-H2 bond generally increases at all hydration levels except for the dihydrate. With addition of SUA to SA•AM and SA•DMA, the LBO values of the pre-existing covalent bonds of SUA-contained clusters are higher than those of the clusters without SUA at all hydration levels except for the sixth hydration. This indicates that, although addition of SUA to

the two hydrated clusters does not result in additional proton transfer, the presence of SUA enhances the covalent bonds at the hydration levels of 0 to 5. The electron and the potential energy densities at BCPs of the N-H bonds are somewhat higher and lower, respectively, in the SUA-containing clusters than in those without SUA for most hydration cases (Tables S2 and S3).

Addition of SUA to SA•base results in cleavage of the hydrogen bond between the base and SA molecules (Figures 1b, 2b and 3b). Note that the carbon chain of SUA tends to bend accordingly as the hydration degree increases, because the carboxylic groups at the two ends of the carbon chain are involved in hydrogen bonding. As expected, the number of hydrogen bonds by AM in SA•AM•SUA clusters increases with the hydration degree, which is always equal or larger than that of the corresponding clusters without SUA and is closely related to the free energy changes of SUA addition to SA•AM clusters (see detailed discussions below on the energetics). For the DMA-containing clusters, the nitrogen atom is saturated by two hydrogen bonds, and the presence of the two free methyl groups likely corresponds to another factor affecting the stability (Ortega et al., 2012). The complexity of the cluster structures is partially ascribed by intramolecular hydrogen bonding associated with SUA, as illustrated by SA•AM•SUA•W, SA•DMA•SUA•W, or SA•AM•DMA•SUA•$(W)_5$ (Figures 1b, 2b and 3b).

### 3.2 ENERGETICS

The stepwise hydration free energies for the clusters, along with the number of water molecules in the clusters, are presented in Figure 5a and Table 2. For SA•AM and SA•DMA with up to five water molecules, the free energies are in agreement with those by Henschel et al. (2014) using the RICC2/aug-cc-pV(T+d)Z level for sulfur and the RICC2/aug-cc-pVTZ level for all other atoms, but differ from those by Loukonen et al. (2010) at the RI-MP2/aug-cc-pV(T+d)Z level of theory. Note that the structures of the hydrates in this study and Henschel et al. are different from

256 those of Loukonen et al. (2010), explaining the differences in the energies among the various
257 studies.

258 Figure 5a shows that the stepwise hydration energies are negative at most hydration degrees,
259 suggesting that hydration stabilizes the clusters. Without SUA, the fifth hydration of SA•AM and
260 SA•DMA•AM and the sixth hydration of SA•DMA exhibit positive or nearly zero one step
261 hydration free energies. These endergonic steps are ascribed because of the saturation by water
262 molecules of the SA•base clusters (Henschel et al., 2013). For SUA-containing clusters, the
263 addition of one more water molecule increases the free energy, resulting in a larger positive
264 hydration energy. For example, the one step free energies are 2.99, 3.24 and 1.32 kcal $mol^{-1}$ for
265 the fifth hydration for SA•AM•SUA, the fourth hydration for SA•DMA•SUA, the third hydration
266 of SA•DMA•AM•SUA, respectively. The large increases in free energies for SA•AM•SUA and
267 SA•DMA•SUA are explained by structural rearrangement. The positive one-step hydration energy
268 for the third hydration of SA•DMA•AM•SUA is likely because of the formation of the stable
269 dihydrate.

270 The relative changes in the free energy due to addition of SUA to the SA•base clusters are
271 depicted along with hydration degree (Figure 5b). The free energy changes for addition of SUA
272 are negative, confirming that this process is energetically favorable. For all hydration levels except
273 the fourth one, the free energy changes for the SA•DMA cluster by SUA addition are more
274 negative than that for the SA•AM cluster, suggesting that the addition of SUA to SA•DMA is more
275 favorable than that to SA•AM. The largest change in the free energy (-7.15 kcal $mol^{-1}$) between
276 SA•AM•SUA and SA•AM occurs at the fourth hydration step, which is attributable to the structure
277 change due to SUA addition, i.e., an additional hydrogen bond formed on AM in the fourth hydrate
278 of SA•AM•SUA. However, such a hydrogen bond is absent in the SA•AM cluster until the fifth

hydration (Figure 1). The largest negative free energy change (-9.86 kcal $mol^{-1}$) in SA•DMA corresponds to the unhydrated form. The strong hydrogen bonds between DMA and the two acids formed in the unhydrated SA•DMA•SUA cluster undergo cleavage due to water uptake, leading to a smaller free energy difference between the SA•DMA•SUA and SA•DMA clusters with hydration. In addition, stabilization by hydration for the SA•base clusters is weakened by addition of SUA, particularly for the SA•DMA and SA•DMA•AM clusters, with much smaller hydration energies for SA•DMA•SUA and SA•DMA•AM•SUA than the corresponding clusters without SUA (Fig. 5a). The effects of SUA addition are relevant to the hydration degree and the base types, implying a synergetic interaction in the multi-component clusters.

The role of SUA in the subsequent growth of the SA•base clusters was examined by comparing the differences in free energies for adding SA to SA•DMA and SA•DMA•SUA. Computations were also performed for the unhydrated $(SA)_2$•DMA, $(SA)_3$•DMA and $(SA)_2$•DMA•SUA clusters (Table 6). The optimized clusters containing more than one SA molecules are depicted in Figure 6. The free energies of SA addition to SA•DMA and $(SA)_2$•DMA are -10.5 and -6.1 kcal $mol^{-1}$, respectively. The free energy for adding SA to SA•DMA•SUA is -5.14 kcal $mol^{-1}$, higher than that of SA addition to SA•DMA. However, with hydration (i.e., $(SA)_2$•DMA•SUA•(W)x), the free energies for adding SA to SA•DMA•SUA•(W)x clusters are negative except for the hydration with six water molecules (Table 2), indicating that SA addition to SA•DMA•SUA is also energetically favorable. In addition, addition of SA to SA•DMA•SUA results in formation of strong hydrogen bond (i.e., -19.1 kcal $mol^{-1}$). Therefore, the clusters containing both the base and organic acid (e.g., SA•DMA•SUA) are capable of further binding with acid molecules to promote the subsequent growth.

### 3.3 HYDRATION PROFILES

The equilibrium hydrate distributions were calculated for the SA•base clusters with and without the presence of SUA. Figure 7 displays the relative hydrate distributions under three typical atmospheric RH values, i.e., 20%, 50% and 80%. The SA•base cluster shows an increasing hydration with increasing RH, although the different clusters exhibit distinct characteristics in the hydrate distribution.

Our results for the SA•AM hydrate distribution are consistent with the previous studies (Loukonen et al., 2010; Henschel et al., 2014), showing that the hydrate distribution of SA•AM is sensitive to RH (Figure 7a). The completely dry SA•AM cluster dominates the hydrate distribution under low RH (<40%), while the trihydrate is most prevalent as RH exceeds 40% because of higher stability of the trihydrate than the monohydrate and dihydrate. Since the change in the free energies is almost identical for addition of 1 or 2 water molecules, the SA•DMA clusters of the unhydrated form, monohydrate, and dihydrate are evenly distributed (Figure 7b) and account for 85% of the total population at all RH levels. The peak of the hydrate distribution for SA•DMA shows a continuous shift from the unhydrated cluster to dihydrate with increasing RH. The SA•DMA•AM cluster tends to be dehydrated, as reflected by the fact that the relative population of dry SA•DMA•AM clusters exceeds 50% even under highly humid conditions (Figure 7c). Hence, addition of DMA or AM considerably lowers the hydrophilicity of SA•AM or SA•DMA. The dehydration trend of the SA•DMA•AM cluster in our work is consistent with the previous investigations,[31] in which the base-containing clusters with SA were found to be less hydrophilic than the SA clusters.

Addition of SUA alters the hydrate distribution of the SA•base clusters. For example, the hydrate distribution is broader for SA•AM•SUA than for SA•AM (Figure 7a,d), with a

considerably high population of the fourth hydrate for SA•AM•SUA at high RH to promote hydration. The broader hydrate distribution is consistent with the more negative hydration energy at the fourth hydration step for SA•AM•SUA for SA•AM. However, the peaks of the distribution exhibit a similar pattern with varying RH for SA•AM and SA•AM•SUA, i.e., with unhydrated and trihydrate clusters as the most populated forms. The hydrate distributions for SA•DMA•SUA and SA•DMA exhibit distinct characteristics. In the presence of SUA, over 80% of the clusters exist in a dry state independent on RH (Figure 7e), indicating that hydration of SA•DMA•SUA is less favorable than that of SA•DMA. The hydrate distribution peak for SA•DMA•SUA at the unhydrated cluster is consistent with that addition of SUA greatly reduces the free energy of the dry clusters and the changes in hydration free energy are relatively small at all hydration levels. The SA•DMA•AM•SUA clusters are likely dehydrated or hydrated with two water molecules dependent on RH (Figure 7f), as the distribution peak shifts between the unhydrated (RH < 70%) and the dihydrate (RH >70%) clusters and does not exhibit a peak on monohydrate at any RH level. Clearly, hydration is more favorable for SA•DMA•AM•SUA than for SA•DMA•AM.

The hydration profiles are shown in Figure 8 as functions of RH for the clusters with SA•base. The maximal numbers of water molecules for SA•AM, SA•DMA, and SA•DMA•AM are 2.7, 1.7, and 0.9, respectively, as RH approaches 100%. The calculated degrees of hydration for SA•AM and SA•DMA are slightly higher by this study than those by Henschel et al. (2014) Addition of SUA considerably enhances the hydrophilicity of SA•AM and SA•DMA•AM, leading to high degrees of hydration for SUA-containing clusters. In contrast, the number of water molecules bound to SA•DMA is greatly reduced with SUA addition, since the most populated cluster of SA•DMA•SUA is unhydrated for different RH (Figure 7e).

## 3.4 ATMOSPHERIC IMPLICATIONS

Addition of SUA to SA•base is energetically favorable (Figure 5b), as reflected by large negative free energies. The estimated cluster concentrations using equation (9) and the atmospherically relevant concentrations of the precursor species are $10^{-3}$ ~$10^{2}$ $cm^{-3}$ for SUA•SA•DMA (Table 6), suggesting that SUA likely contributes to the further growth of the SA•base clusters. The calculated ratios of [SA•X•SUA]/[$(SA)_2$•X] (X denotes AM, DMA, water molecule, or none) under atmospherically relevant concentrations are presented in Table 7. The estimated ratio of [SA•DMA•SUA] to [$(SA)_2$•DMA] is in the range from 3:1 to 3000:1 under atmospherically relevant concentrations for the precursor species, i.e., [SUA]/[SA] in the range from 10:1 to $10^4$:1, indicating that SA•DMA•SUA is prevalent in the atmosphere. The ratios of [SA•SUA]/[$(SA)_2$] and [SA•W•SUA]/[$(SA)_2$•W] are both higher than $10^3$:1, indicating that the SUA-containing clusters are prevalent for both unhydrated and hydrated SA clusters with one water molecule. While sulfuric acid dimer is believed to be an important precursor for NPF (Zhang et al., 2012), our study shows that SUA, which is one of most abundant dicarboxylic acids in atmosphere, competes with the formation and further growth of sulfuric acid dimer because of the strong interaction of SUA with SA to form the unhydrated or hydrated clusters. The effect of SUA on the formation and further growth of sulfuric acid dimer is more pronounced than that by ketodiperoxy acid (Elm et al., 2016b). Fig. 9 depicts the relative stability of cluster formation from the interaction among SUA, SA, base, and W molecules, showing SA•DMA as the most stable dimer and $(SA)_2$•DMA as most stable trimer, following by SA•DMA•SUA.

It should be pointed out that steady-state equilibrium for pre-nucleation clusters is rarely established under atmospheric conditions, because of continuous forward reactions by adding monomers to form larger clusters during NPF. Clearly, the ability whether a cluster grows to form

a nanoparticle is dependent on the competition between the forward reaction by adding a monomer and the backward reaction by losing a monomer (evaporation) at each intermediate step. While the evaporation rate relies on the thermodynamic stability of the cluster, the forward rate constant is kinetically controlled, dependent on the interaction (i.e., the natural charges and dipole moments) and kinetical energies between the colliding cluster and monomer (Zhang et al., 2012). For neutral clusters, electrostatically-induced dipole-dipole interaction plays a key role in facilitating the forward reaction rate. The presence of organic acids typically increases the dipole moment of clusters (Zhao et al., 2009).

## 4. CONCLUSIONS

We have investigated the molecular interactions between SUA and SA•base clusters in the presence of hydration, including AM and DMA. Addition of SUA to SA•base is energetically favorable at all hydration levels, suggesting that SUA likely stabilizes the SA•base clusters and their hydrates. In addition, SUA addition promotes proton transfer in the SA•base clusters, which is confirmed by formation of new covalent bonds and relocation of the high LOL value from the SA side to the AM side and a shift from positive to negative for the Laplacian of electron density. The presence of SUA in SA•AM and SA•DMA clusters generally strengthens the existing covalent bonds in SA•base•SUA•$(W)_n$ clusters at the various hydration levels, since the LBO values of the covalent bonds in SUA-containing clusters are higher than those in the clusters without SUA. The hydrate distribution is broader for SA•AM•SUA than for SA•AM. Also, the peak in the distribution of SA•DMA•AM•SUA hydrates occurs at the two-water molecule level under high RH, but the peak in the distribution for SA•DMA•AM corresponds to the unhydrated cluster. The peak hydrate distribution shifts toward a larger number of water molecules in SUA-containing clusters than in clusters without SUA, suggesting that the addition of SUA enhances the hydrophilicity of SA•AM

and SA•DMA•AM. However, the presence of SUA causes dehydration to the SA•DMA clusters, since the most prevalent cluster for SA•DMA•SUA is in a dry state. At equilibrium and atmospherically typical abundances of SUA and SA, SUA•SA•base (AM or DMA) is the most dominant form among the three-molecule clusters, indicating that SUA competes with SA for the growth of the SA•base dimers.

Our results indicate that the multi-component molecular interaction involving organic acids, sulfuric acid, and base species promotes NPF in the atmosphere, particularly under polluted environments because of the co-existence of elevated concentrations of these nucleation precursors. Future studies are necessary to assess the kinetics (forward and reverse rates) and potential energy surface for the cluster growth, in order to develop physically-based parameterizations of NPF in atmospheric models.

## SUPPLEMENTARY MATERIAL

Supplementary material contains additional relief maps for the sulfuric acid-base clusters and lists of topological properties for the most stable conformers of each cluster categories.

## ACKNOWLEDGMENTS

This work was supported by National Natural Science Foundation of China (41675122, 41425015, U1401245, and 41373102), Science and Technology Program of Guangzhou City (201707010188), Team Project from the Natural Science Foundation of Guangdong Province, China (S2012030006604), Special Program for Applied Research on Super Computation of the NSFC-Guangdong Joint Fund (the second phase), National Super-computing Centre in Guangzhou (NSCC-GZ), and Robert A. Welch Foundation (A-1417). The research was partially conducted with the advanced computing resources provided by Texas A&M High Performance

414 Research Computing. The authors acknowledged the Laboratory for Molecular Simulations at
415 Texas A&M University.
416

## References


Andreae, M. O., Rosenfeld, D., Artaxo, P., Costa, A. A., Frank, G. P., Longo, K. M., and Silva-Dias, M. A. F.: Smoking rain clouds over the Amazon, Science, 303, 1337–1342, 2004.

Anderson, K. E., Siepmann, J. I., McMurry, P. H., and VandeVondele, J.: Importance of the Number of Acid Molecules and the Strength of the Base for Double-Ion Formation in (H2SO4)m•Base•(H2O)6 Clusters, J. Am. Chem. Soc., 130, 14144–14147, https://doi.org/10.1021/ja8019774, 2008.

Al Natsheh, A., Nadykto, A. B., Mikkelsen, K. V., Yu, F., and Ruuskanen, J.: Sulfuric acid and sulfuric acid hydrates in the gas phase: A DFT investigation, J. Phys. Chem. A, 108, 8914–8929, https://doi.org/10.1021/jp048858o, 2004.

Bianchi, F., Tröstl, J., Junninen, H., Frege, C., Henne, S., Hoyle, C. R., Molteni, U., Herrmann, E., Adamov, A., Bukowiecki, N., Chen, X., Duplissy, J., Gysel, M., Hutterli, M., Kangasluoma, J., Kontkanen, J., Kürten, A., Manninen, H. E., Münch, S., Peräkylä, O., Petäjä, T., Rondo, L., Williamson, C., Weingartner, E., Curtius, J., Worsnop, D. R., Kulmala, M., Dommen, J., and Baltensperger, U.: New particle formation in the free troposphere: A question of chemistry and timing, Science, 352, 1109–1112, https://doi.org/10.1126/science.aad5456, 2016.

Blower, P. G., Ota, S. T., Valley, N. A., Wood, S. R., and Richmond, G. L.: Sink or Surf: Atmospheric Implications for Succinic Acid at Aqueous Surfaces, J. Phys. Chem. 117, 7887–7903, https://doi.org/10.1021/jp405067y, 2013.

Cai, R., and Jiang, J.: A new balance formula to estimate new particle formation rate: reevaluating the effect of coagulation scavenging, Atmos. Chem. Phys., 17, 12659-12675, https://doi.org/10.5194/acp-17-12659-2017, 2017.

Decesari, S., Facchini, M. C., Fuzzi, S., and Tagliavini, E., Characterization of water-soluble organic compounds in atmospheric aerosol: A new approach, J. Geophys. Res. Atmos., 105, 1481-1489, https://doi.org/10.1029/1999JD900950, 2000.

DePalma, J. W., Bzdek, B. R., Doren, D. J., and Johnston, M. V.: Structure and energetics of nanometer size clusters of sulfuric acid with ammonia and dimethylamine, J. Phys. Chem. A 116, 1030–1040, https://doi.org/10.1021/jp210127w, 2012.

Ding, C.-G., Laasonen, K., and Laaksonen, A.: Two sulfuric acids in small water clusters, J. Phys. Chem. 107, 8648–8658, https://doi.org/10.1021/jp022575j, 2003.

Elm, J., Bilde, M., and Mikkelsen, K. V.: Assessment of density functional theory in predicting structures and free energies of reaction of atmospheric prenucleation clusters, J. Chem. Theory and Comp., 8, 2071–2077, https://doi.org/10.1021/ct300192p, 2012.

Elm, J., Kurten, T., Bilde, M., and Mikkelsen, K. V.: Molecular interaction of pinic acid with sulfuric acid: exploring the thermodynamic landscape of cluster growth, J. Phys. Chem. A, 118, 7892-7900, https://doi.org/10.1021/jp503736s (2014).

Elm, J., Jen, C. N., Kurtén, T., and Vehkamäki, H.: Strong hydrogen bonded molecular interactions between atmospheric diamines and sulfuric acid, J. Phys. Chem., 120, 3693–3700, https://doi.org/10.1021/acs.jpca.6b03192, 2016a.

Elm, J., Myllys, N., Luy, J.-N., Kurtén, T., and Vehkamäki, H.: The Effect of Water and Bases on the Clustering of a Cyclohexene Autoxidation Product C6H8O7 with Sulfuric Acid, J. Phys. Chem., 120, 2240–2249, https://doi.org/10.1021/acs.jpca.6b00677, 2016b.

Elm, J., Myllys, N., and Kurtén, T.: What is required for highly oxidized molecules to form clusters with sulfuric acid? J. Phys. Chem., 121 (23), 4578-4587, doi: 10.1021/acs.jpca.7b03759, 2017.

461 Erupe, M. E., Viggiano, A. A., and Lee, S.-H.: The effect of trimethylamine on atmospheric
462 nucleation involving H2SO4, Atmos. Chem. Phys., 11, 4767-4775,
463 https://doi.org/10.5194/acp-11-4767-2011, 2011.
464 Espinosa, E., Molins, E., and Lecomte, C.: Hydrogen bond strengths revealed by topological
465 analyses of experimentally observed electron densities, Chem. Phys. Lett. 285, 170-173,
466 https://doi.org/10.1016/S0009-2614(98)00036-0, 1998.
467 Fan, J., Zhang, R., Li, G., and Tao, W.-K.: Effects of aerosols and relative humidity on cumulus
468 clouds, J. Geophys. Res., 112, D14204, https://doi.org/10.1029/2006JD008136, 2007.
469 Frisch, M. J., Trucks, G. W., Schlegel, H. B., Scuseria, G. E., Robb, M. A., Cheeseman, J. R.,
470 Scalmani, G., Barone, V., Petersson, G. A., Nakatsuji, H., Li, X., Caricato, M., Marenich, A.,
471 Bloino, J., and Janesko, R. G. B. G., Mennucci, B., Hratchian, H. P., Ortiz, J. V., Izmaylov,
472 A. F., Sonnenberg, J. L., Williams-Young, D., Ding, F., Lipparini, F., Egidi, F., Goings, J.,
473 Peng, B., Petrone, A., Henderson, T., Ranasinghe, D., Zakrzewski, V. G., Gao, J., Rega, N.,
474 Zheng, G., Liang, W., Hada, M., Ehara, M., Toyota, K., Fukuda, R., Hasegawa, J., Ishida, M.,
475 Nakajima, T., Honda, Y., Kitao, O., Nakai, H., Vreven, T., Throssell, K., Montgomery Jr., J.
476 A., Peralta, J. E., Ogliaro, F., Bearpark, M., Heyd, J. J., Brothers, E., Kudin, K. N., Staroverov,
477 V. N., Keith, T., Kobayashi, R., Normand, J., Raghavachari, K., Rendell, A., Burant, J. C.,
478 Iyengar, S. S., Tomasi, J., Cossi, M., Millam, J. M., Klene, M., Adamo, C., Cammi, R.,
479 Ochterski, J. W., Martin, K. R. L., Morokuma, Farkas, O., Foresman, J. B., and Fox, D. J.:
480 Gaussia, Gaussian 09, Revision A.02 (Gaussian, Inc., Wallingford CT, 2009),
481 Guo, S., Hu, M., Zamora, M. L., Peng, J., Shang, D., Zheng, J., Du, Z., Wu, Z., Shao, M., Zeng,
482 L., Molina, M.J., and Zhang, R.: Elucidating severe urban haze formation in China, Proc. Natl.
483 Acad. Sci. USA, 111, 17373–17378, https://doi.org/10.1016/10.1073/pnas.1419604111, 2014.

484 Hanson, D. R., and Eisele, F. L.: Acid–base chemical reaction model for nucleation rates in the
485 polluted atmospheric boundary layer, J. Geophys. Res. Atmos., 107, 18713-18718,
486 https://doi.org/10.1073/pnas.1210285109, 2002.
487 Henschel, H., Ortega, I. K., Kupiainen, O., Olenius, T., Kurtén, T., and Vehkamäki, H.: Hydration
488 of pure and base-Containing sulfuric acid clusters studied by computational chemistry
489 methods, AIP Conference Proceedings, 1527, 218-221, https://doi.org/10.1063/1.4803243,
490 2013.
491 Henschel, H., T. Kurtén, and Vehkamäki, H.: Hydration of Atmospherically Relevant Molecular
492 Clusters: Computational Chemistry and Classical Thermodynamics, J. Phys. Chem., 120,
493 2599–2611, https://doi.org/10.1021/jp500712y, 2016.
494 Henschel, H., Navarro, J. C., Yli-Juuti, T., Kupiainen-Maatta, O., Olenius, T., Ortega, I. K., Clegg,
495 S. L., Kurten, T., Riipinen, I., and Vehkamaki, H.: Hydration of atmospherically relevant
496 molecular clusters: Computational chemistry and classical thermodynamics, J. Phys. Chem.
497 A, 118, 2599-2611, https://doi.org/10.1021/jp500712y, 2014.
498 Ho, K. F., Cao, J. J., Lee, S. C., Kawamura, K., Zhang, R. J. , Chow, J. C., and Watson, J.
499 G.: Dicarboxylic acids, ketocarboxylic acids, and dicarbonyls in the urban atmosphere of
500 China, J. Geophys. Res., 112, D22S27, https://doi.org/10.1029/2006JD008011, 2007.
501 Hsieh, L.-Y., Kuo, S.-C., Chen, C.-L., and Tsai, Y. I.: Origin of Low-molecular-weight
502 Dicarboxylic Acids and their Concentration and Size Distribution Variation in Suburban
503 Aerosol, Atmos. Environ., 41, 6648–6661, https://doi.org/10.1016/j.atmosenv.2007.04.014
504 2007.
505 IPCC, Climate Change 2013: The Physical Science Basis. Contribution of Working Group I to the
506 Fifth Assessment Report of the Intergovernmental Panel on Climate Change (Cambridge

University Press, Cambridge, United Kingdom and New York, NY, USA: http://www.ipcc.ch/report/ar5/wg1/, 2013).

Kawamura, K., and Kaplan, I. R.: Motor exhaust emissions as a primary source for dicarboxylic acids in Los Angeles ambient air, Environ. Sci. Technol., 21, 105-110, 1987.Legrand, M., Preunkert, S., Galy-Lacaux, C., Liousse, C., and Wagenbach, D.: J. Geophys. Res.: Atmospheric year‐round records of dicarboxylic acids and sulfate at three French sites located between 630 and 4360 m elevation, Atmos. 110, https://doi.org/10.1029/2004JD005515, 2005.

Kuang, C., Riipinen, I., Sihto, S.-L., Kulmala, M., McCormick, A. V., and McMurry, P. H.: An improved criterion for new particle formation in diverse atmospheric environments, Atmos. Chem. Phys., 10, 8469–8480, doi:10.5194/acp-10-8469-2010, 2010.

Kulmala, M. and Kerminen, V. M.: On the formation and growth of atmospheric nanoparticles, Atmos. Res., 90, 132–150, https://doi.org/10.1016/j.atmosres.2008.01.005, 2008.

Kurtén, T., Sundberg, M. R., Vehkamäki, H., Noppel, M., Blomqvist, J., and Kulmala, M.: Ab initio and density functional theory reinvestigation of gas-phase sulfuric acid monohydrate and ammonium hydrogen sulfate, J. Phys. Chem. https://doi.org/110, 7178–7188, 10.1021/jp0613081, 2006.

Lane, J. R., Contreras-García, J., Piquemal, J.-P., Miller, B. J., and Kjaergaard, H. G.: Are bond critical points really critical for hydrogen bonding? J. Chem. Theory and Comp. 9, 3263–3266, https://doi.org/10.1021/ct400420r, 2013.

Lee, S. H., Reeves, J. M., Wilson, J. C., Hunton, D. E., Vig- giano, A. A., Miller, T. M., Ballenthin, J. O., and Lait, L. R.: Particle formation by ion nucleation in the upper tro- posphere and lower stratosphere: Science, 301, 1886–1889, https://doi.org/10.1126/science.1087236, 2003.

529 Leverentz, H. R., Siepmann, J. I., Truhlar, D. G., Loukonen, V., and Vehkamäki, H.: Energetics
530 of atmospherically implicated clusters made of sulfuric acid, ammonia, and dimethyl amine,
531 J. Phys. Chem. A, 117, 3819–3825, https://doi.org/10.1021/jp402346u, 2013.
532 Li, G., Wang, Y., and Zhang, R.: Implementation of a two-moment bulk microphysics scheme to
533 the WRF model to investigate aerosol-cloud interaction, J. Geophys. Res. 113, D15211,
534 https://doi.org/10.1029/2007JD009361, 2008.
535 Loukonen, V., Kurtén, T., Ortega, I. K., Vehkamäki, H., Pádua, A. A. H., Sellegri, K., Kulmala,
536 M.: Enhancing effect of dimethylamine in sulfuric acid nucleation in the presence of water –
537 a computational study, Atmos. Chem. Phys., 10, 4961-4974, https://doi.org/10.5194/acp-10-
538 4961-2010, 2010.
539 Lu, T., and Chen, F.: Multiwfn: A multifunctional wavefunction analyzer, J. Comput. Chem. 33,
540 580-592, https://doi.org/10.1002/jcc.22885, 2012.
541 Lu, T., and Chen, F.: Bond order analysis based on the Laplacian of electron density in fuzzy
542 overlap space, J. Phys. Chem. A, 117, 3100–3108, https://doi.org/10.1021/jp4010345, 2013.
543 McGraw, R., and Zhang, R.: Multivariate analysis of homogeneous nucleation rate measurements:
544 I. Nucleation in the p-toluic acid/sulfuric acid/water system, J. Chem. Phys. 128, 064508,
545 https://doi.org/10.1063/1.2830030, 2008.
546 Merikanto, J., Spracklen, D. V., Mann, G. W., Pickering, S. J., and Carslaw, K. S.: Impact of
547 nucleation on global CCN, Atmos. Chem. Phys., 9, 8601-8616, https://doi.org/10.5194/acp-
548 9-8601-2009, 2009.
549 Nadykto, A. B., and Yu, F.: Strong hydrogen bonding between atmospheric nucleation precursors
550 and common organics, Chem. Phys. Lett., 435, 14-18,
551 https://doi:.org/10.1016/j.cplett.2006.12.050, 2007.

552 Nadykto, A.B., Yu, F., Jakovleva, M.V., Herb, J., and Xu, Y.: Amines in the Earth's Atmosphere:
553 A Density Functional Theory Study of the Thermochemistry of Pre-Nucleation Clusters,
554 Entropy, 13, 554–569, https://doi.org/10.3390/e13020554, 2011.
555 Nieminen, T., H. E. Manninen, S. L. Sihto, T. Yli-Juuti, I. R. L. Mauldin, T. Petäjä, I. Riipinen, V.
556 M. Kerminen, and Kulmala M.: Connection of Sulfuric Acid to Atmospheric Nucleation in
557 Boreal Forest, Environmental Science & Technology, 43(13), 4715-4721,
558 doi:10.1021/es803152j, 2009.
559 Qiu, C., and Zhang, R.: Multiphase chemistry of atmospheric amines, Phys. Chem. Chem. Phys.,
560 15, 5738-5752, https://doi.org/10.1039/C3CP43446J, 2013.
561 Ortega, I. K., Kupiainen, O., Kurtén, T., Olenius, T., Wilkman, O., McGrath, M. J., Loukonen, V.,
562 and Vehkamäki, H.: From quantum chemical formation free energies to evaporation rates,
563 Atmos. Chem. Phys., 12, 225-235, https://doi.org/10.5194/acp-12-225-2012, 2012
564 Riccobono, F., Schobesberger, S., Scott, C. E., Dommen, J., Ortega, I. K., Rondo, L., Almeida, J.,
565 Amorim, A., Bianchi, F., Breitenlechner, M., David, A., Downard, A., Dunne, E. M., Duplissy,
566 J., Ehrhart, S., Flagan, R. C., Franchin, A., Hansel, A., Junni- nen, H., Kajos, M., Keskinen,
567 H., Kupc, A., Kürten, A., Kvashin, A. N., Laaksonen, A., Lehtipalo, K., Makhmutov, V.,
568 Mathot, S., Nieminen, T., Onnela, A., Petäjä, T., Praplan, A. P., Santos, F. D., Schallhart, S.,
569 Seinfeld, J. H., Sipilä, M., Spracklen, D. V., Stozhkov, Y., Stratmann, F., Tomé, A.,
570 Tsagkogeorgas, G., Vaattovaara, P., Viisanen, Y., Vrtala, A., Wagner, P. E., Weingart- ner,
571 E., Wex, H., Wimmer, D., Carslaw, K. S., Curtius, J., Donahue, N. M., Kirkby, J., Kulmala,
572 M., Worsnop, D. R., and Baltensperger, U.: Oxidation products of biogenic emissions
573 contribute to nucleation of atmospheric particles, Science 344, 717-721,
574 https://doi.org/10.1126/science.1243527, 2014.

Tröstl, J., Chuang, W. K., Gordon, H., Heinritzi, M., Yan, C., Molteni, U., Ahlm, L., Frege, C., Bianchi, F., Wagner, R., Si- mon, M., Lehtipalo, K., Williamson, C., Craven, J. S., Du- plissy, J., Adamov, A., Almeida, J., Bernhammer, A.-K., Bre- itenlechner, M., Brilke, S., Dias, A., Ehrhart, S., Flagan, R. C., Franchin, A., Fuchs, C., Guida, R., Gysel, M., Hansel, A., Hoyle, C. R., Jokinen, T., Junninen, H., Kangasluoma, J., Kesk- inen, H., Kim, J., Krapf, M., Kürten, A., Laaksonen, A., Lawler, M., Leiminger, M., Mathot, S., Möhler, O., Nieminen, T., On- nela, A., Petäjä, T., Piel, F. M., Miettinen, P., Rissanen, M. P., Rondo, L., Sarnela, N., Schobesberger, S., Sengupta, K., Sip- ilä, M., Smith, J. N., Steiner, G., Tomè, A., Virtanen, A., Wag- ner, A. C., Weingartner, E., Wimmer, D., Winkler, P. M., Ye, P., Carslaw, K. S., Curtius, J., Dommen, J., Kirkby, J., Kulmala, M., Riipinen, I., Worsnop, D. R., Donahue, N. M., and Bal- tensperger, U.: The role of low-volatility organic compounds in initial particle growth in the atmosphere, Nature, 533, 527-531, https://doi.org/10.1038/nature18271, 2016.

Tsona, N. T., Henschel, H., Bork, N., Loukonen, V., and Vehkamäki, H.: Structures, Hydration, and Electrical Mobilities of Bisulfate Ion–Sulfuric Acid–Ammonia/Dimethylamine Clusters: A Computational Study, J. Phys. Chem. A, 119, 9670–9679, https://doi.org/10.1021/acs.jpca.5b03030, 2015.

Wang, L., Khalizov, A.F., Zheng, J., Xu, W., Lal, V., Ma, Y., and Zhang, R.: Atmospheric nanoparticles formed from heterogeneous reactions of organics, Nature Geosci., 3, 238-242, https://doi.org/10.1038/ngeo778, 2010.

Wang, J., Krejci, R., Giangrande, S., Kuang, C., Barbosa, H. M. J., Brito, J., Carbone, S., Chi, X., Comstock, J., Ditas, F., Lavric, J., Manninen, H. E., Mei, F., Moran-Zuloaga, D., Pöhlker, C., Pöh- lker, M. L., Saturno, J., Schmid, B., Souza, R. A. F., Springston, S. R., Tomlinson, J. M., Toto, T., Walter, D., Wimmer, D., Smith, J. N., Kulmala, M., Machado, L. A. T., Artaxo, P.,

598 Andreae, M. O., Petäjä, T., and Martin, S. T.: Amazon boundary layer aerosol concentration
599 sustained by vertical transport during rainfall, Na- ture, 539, 416–419,
600 https://doi.org/10.1038/nature19819, 2016.
601 Wang, C.-Y., Jiang, S., Liu, Y.-R., Wen, H., Wang, Z.-Q., Han, Y.-J., Huang, T., Huang, W.:
602 Synergistic Effect of Ammonia and Methylamine on Nucleation in the Earth's Atmosphere.
603 A Theoretical Study, J. Phys. Chem. A, 122, 3470−3479, https://doi.org/
604 10.1021/acs.jpca.8b0068, 2018.
605 Weber, R. J., P. H. McMurry, R. L. Mauldin III, D. J. Tanner, F. L. Eisele, A. D. Clarke, and
606 Kapustin V. N.: New Particle Formation in the Remote Troposphere: A Comparison of
607 Observations at Various Sites, Geophys. Res. Lett., 26(3), 307-310,
608 doi:10.1029/1998GL900308, 1999.
609 Weber, K. H., Liu, Q., and Tao, F.-M.: Theoretical study on stable small clusters of oxalic acid
610 with ammonia and water, J. Phys. Chem. A, 118, 1451-1468,
611 https://doi.org/10.1021/jp4128226, 2014.
612 Wexler, A.: Vapor pressure formulation for water in range 0 to 100 C. A revision, J. Res. Nat. Bur.
613 Stand. 80A, 775-785, 1976.
614 Xu, Y., Nadykto, A. B., Yu, F., Jiang, L., and Wang, W.: Formation and properties of hydrogen-
615 bonded complexes of common organic oxalic acid with atmospheric nucleation precursors, J.
616 Mol. Struct.: THEOCHEM, 951, 28-33, https://doi.org/10.1016/j.theochem.2010.04.004,
617 2010a.
618 Xu, Y., Nadykto, A. B., Yu, F., Herb, J., and Wang, W.: Interaction between common organic
619 acids and trace nucleation species in the Earth's atmosphere, J. Phys. Chem. A, 114, 387-96,
620 https://doi.org/10.1021/jp9068575, 2010b.

Xu, W., and Zhang, R.: Theoretical investigation of interaction of dicarboxylic acids with common aerosol nucleation precursors, J. Phys. Chem., 116, 4539-4550, https://doi.org/ 10.1021/jp301964u, 2012.

Xu, W., and Zhang, R.: A theoretical study of hydrated molecular clusters of amines and dicarboxylic acids, J. Chem. Phys., 139, 064312, https://doi.org/10.1063/1.4817497, 2013.

Xu, W., Gomez-Hernandez, M., Guo, S., Secrest, J., Marrero-Ortiz, W., Zhang, A. L., and Zhang, R.: Acid-catalyzed reactions of epoxides for atmospheric nanoparticle growth, J. Am. Chem. Soc., 136, 15477−15480, https://doi.org/10.1021/ja508989a, 2014.

Yao, L., Garmash, O., Bianchi, F., Zheng, J., Yan, C., Kontkanen, J., Junninen, H., Mazon, B. S., Ehn, M., Paasonen, P., Sipila, M., Wang, M., Wang, X., Xiao, S., Chen, H., Lu, Y., Zhang, B., Wang, D., Fu, Q., Geng, F., Li, L., Wang, H., Qiao, L., Yang, X., Chen, J., Kerminen, V., Petaja, T., Worsnop, D., Kulmala, M., Wang, L.: Atmospheric new particle formation from sulfuric acid and amines in a Chinese megacity, Science, 361, 278-281, https://doi.org/10.1126/science.aao4839, 2018.

Yu, H., McGraw, R., and Lee, S.-H.: Effects of amines on formation of sub-3 nm particles and their subsequent growth, Geophys. Res. Lett., 39, L02807, https://doi.org/10.1029/2011GL050099, 2012.

Yue, D. L., Hu, M., Zhang, R. Y., Wang, Z. B., Zheng, J., Wu, Z. J., Wiedensohler, A., He, L. Y., Huang, X. F., and Zhu, T.: The roles of sulfuric acid in new particle formation and growth in the mega-city of Beijing, Atmos. Chem. Phys. 10, 4953–4960, https://doi.org/ 10.5194/acp-10-4953-2010, 2010.

642 Yue, D. L., Hu, M., Zhang, R. Y., Wu, Z. J., Su, H., Wang, Z. B., and Wiedensohler, A.: Potential
643 contribution of new particle formation to cloud condensation nuclei in Beijing, Atmos.
644 Environ., 45, 6070-6077, https://doi.org/ 10.1016/j.atmosenv.2011.07.037, 2011.
645 Zhang, R., Suh, I., Zhao, J., Zhang, D., Fortner, E. C., Tie, X., Molina, L. T., and Molina, M. J.:
646 Atmospheric new particle formation enhanced by organic acids, Science, 304, 1487-1490,
647 https://doi.org/10.1126/science.1095139, 2004.
648 Zhang, R., Wang, L., Khalizov, A. F., Zhao, J., Zheng, J., McGraw, R. L., and Molina, L. T.:
649 Formation of nanoparticles of blue haze enhanced by anthropogenic pollution, Proc. Natl.
650 Acad. Sci. USA, 106, 17650-17654, https://doi.org/10.1073/pnas.0910125106, 2009.
651 Zhang, R.: Getting to the critical nucleus of aerosol formation, Science, 328, 1366-1367,
652 https://doi.org/10.1126/science.1189732, 2010.
653 Zhang, R., Khalizov, A.F., Wang, L., Hu, M., Xu, W.: Nucleation and growth of nanoparticles in
654 the atmosphere, Chem. Rev., 112, 1957-2011, https://doi.org/10.1021/cr2001756, 2012.
655 Zhang, R., Wang, G., Guo, S., Zamora, M. L., Ying, Q., Lin, Y., Wang, W., Hu, M., and Wang Y.:
656 Formation of urban fine particulate matter, Chem. Rev., 115, 3803-3855,
657 https://doi.org/10.1021/acs.chemrev.5b00067, 2015.
658 Zhang, H., Kupiainen-Määttä, O., Zhang, X., Molinero, V., Zhang, Y., and Li, Z., The
659 enhancement mechanism of glycolic acid on the formation of atmospheric sulfuric acid–
660 ammonia molecular clusters, J. Chem. Phys., 146, 184308, https://doi.org/10.1063/1.4982929,
661 2017.
662 Zhao, J., Khalizov, A., Zhang, R., and McGraw, R.: Hydrogen bonding interaction of molecular
663 complexes and clusters of aerosol nucleation precursors, J. Phys. Chem. A 113, 680–689,
664 https://doi.org/10.1021/jp806693r, 2009.

Zhu, Y. P., Liu, Y. R., Huang, T., Jiang, S., Xu, K. M., Wen, H., Zhang, W. J., and Huang, W.: Theoretical study of the hydration of atmospheric nucleation precursors with acetic acidJ, Phys. Chem. A, 118, 7959-7974, https://doi.org/10.1021/jp506226z, 2014.

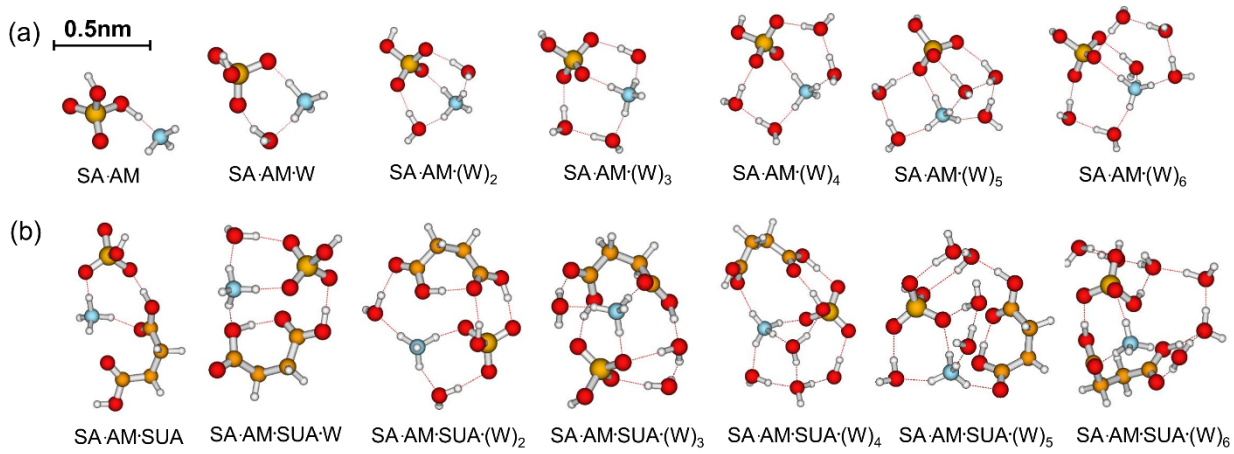


669

670 FIG. 1. Most stable configurations of the hydrated SA•AM clusters and the clusters with one

671 SUA addition. The hydration is with 0-6 water molecules. The sulfur (carbon) atoms are depicted

672 as large (small) yellow balls, oxygen atoms in red, nitrogen atoms in blue, and hydrogen atoms

673 in white. The dash line denotes the hydrogen bond.

674

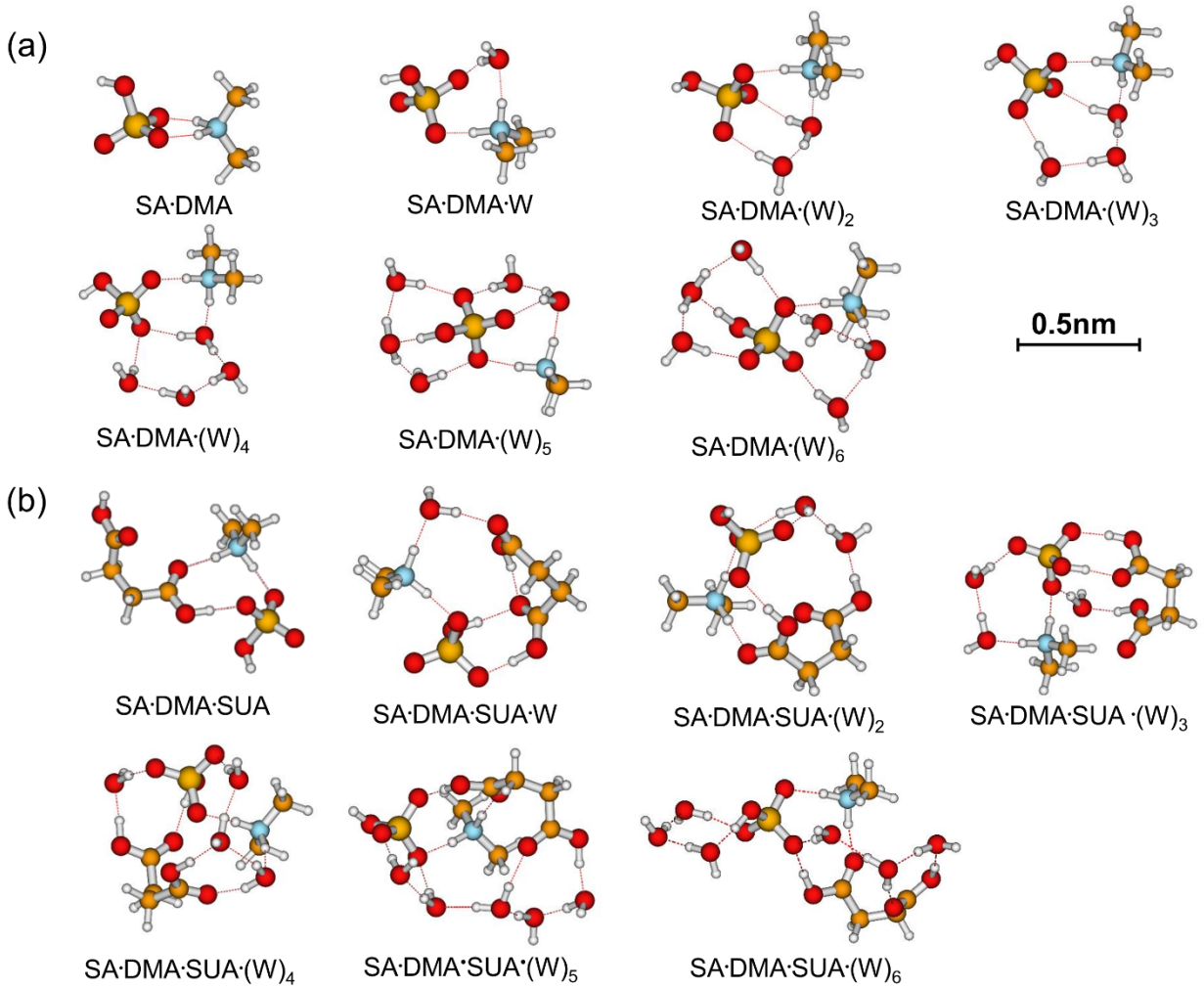


675

676 FIG. 2. Most stable configurations of the hydrated SA•DMA clusters and the clusters with one

677 SUA addition. The hydration is with 0-6 water molecules.

678

679

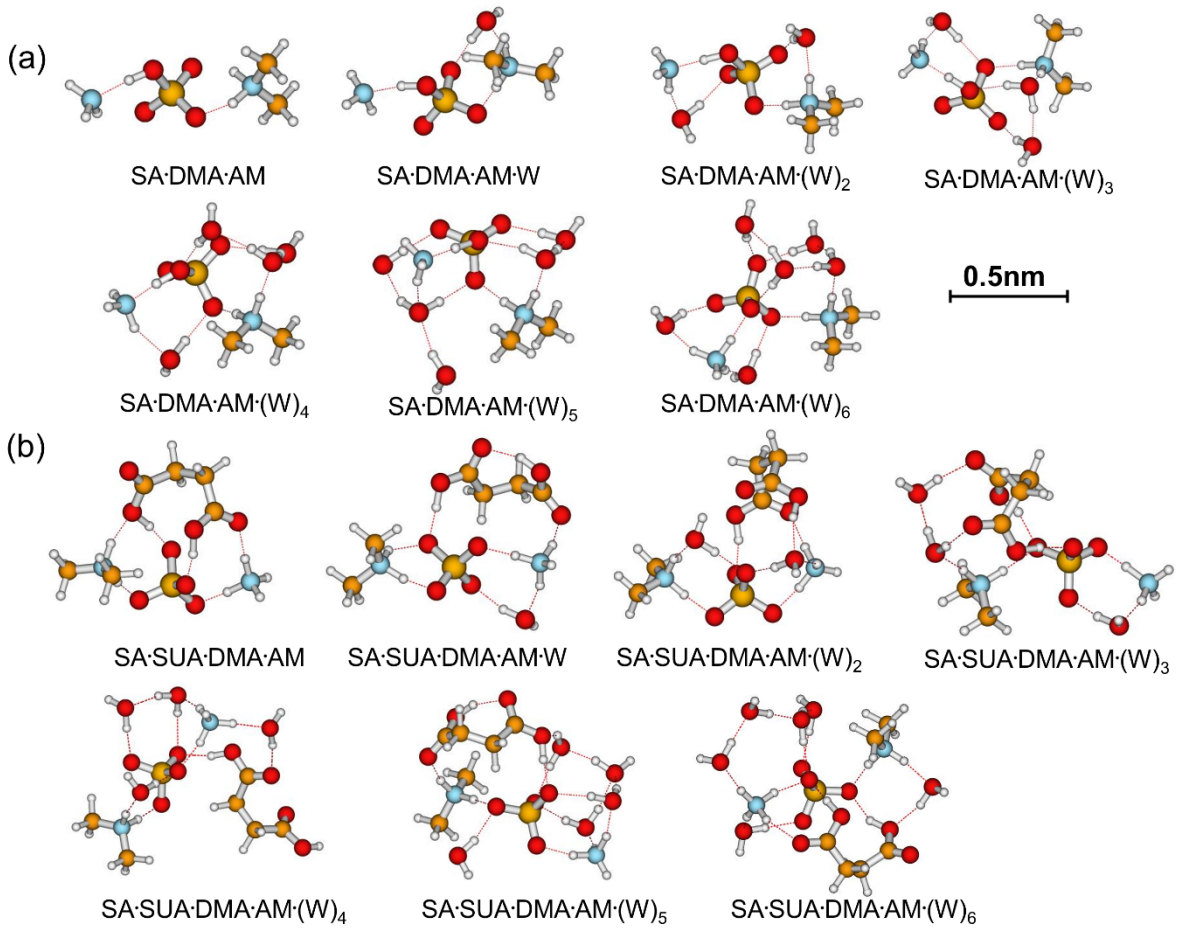


680

681 FIG. 3. Most stable configurations of the hydrated SA•DMA•AM clusters and the clusters with

682 one SUA addition. The hydration is with 0-6 water molecules.

683

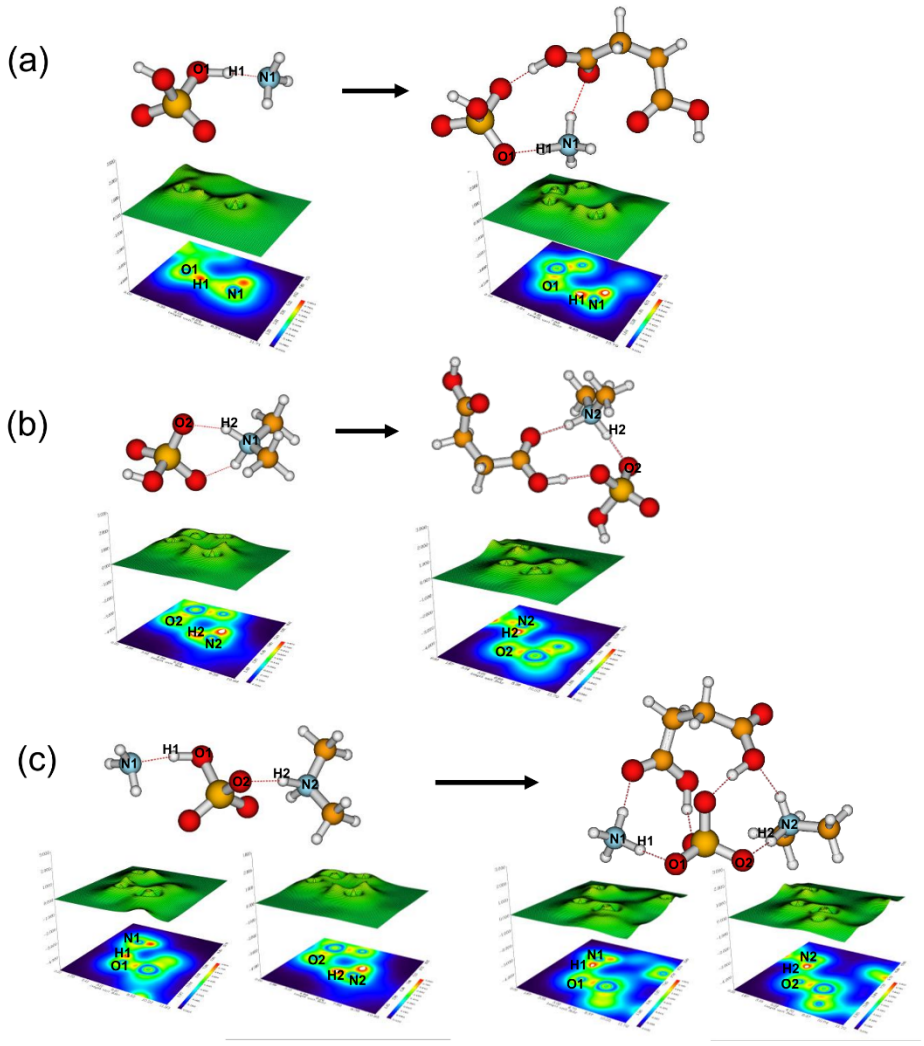


684

685 FIG. 4. Relief maps with the projection of localized orbital locator for clusters of (a) SA•AM and
686 SA•AM•SUA, (b) SA•DMA, SA•DMA•SUA, and (c) SA•DMA•AM and SA•DMA•AM•SUA.
687 Hydrogen bonds are shown as dashed lines. A large LOL value reflects that electrons are greatly
688 localized, indicating the existence of a covalent bond.

689

690

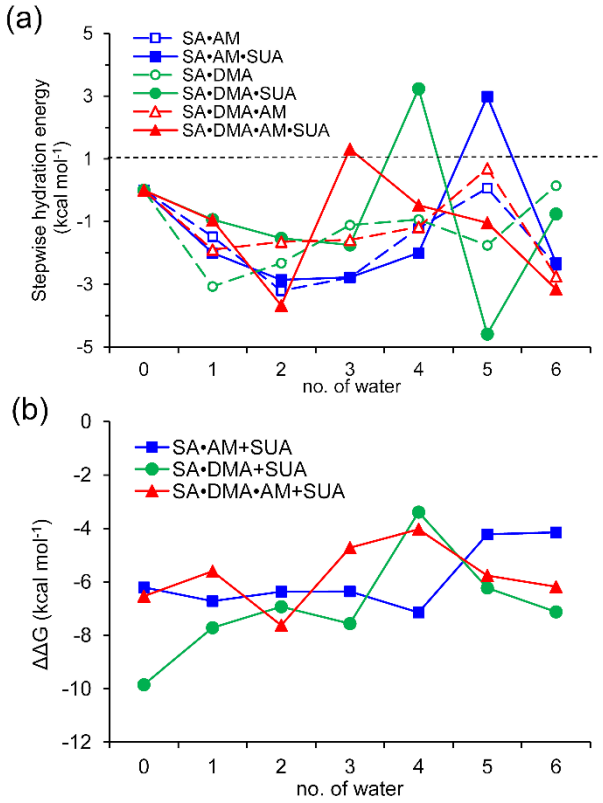


691

692 FIG. 5. Stepwise hydration free energies (a) and the relative Gibbs free energy changes due to

693 addition of one SUA molecule to SA•base clusters (b) at $T$=298.15 K and $p$=1 atm. The free

694 energy is calculated at the PW91PW91/6-311++G(2d, 2p) level.

695

696

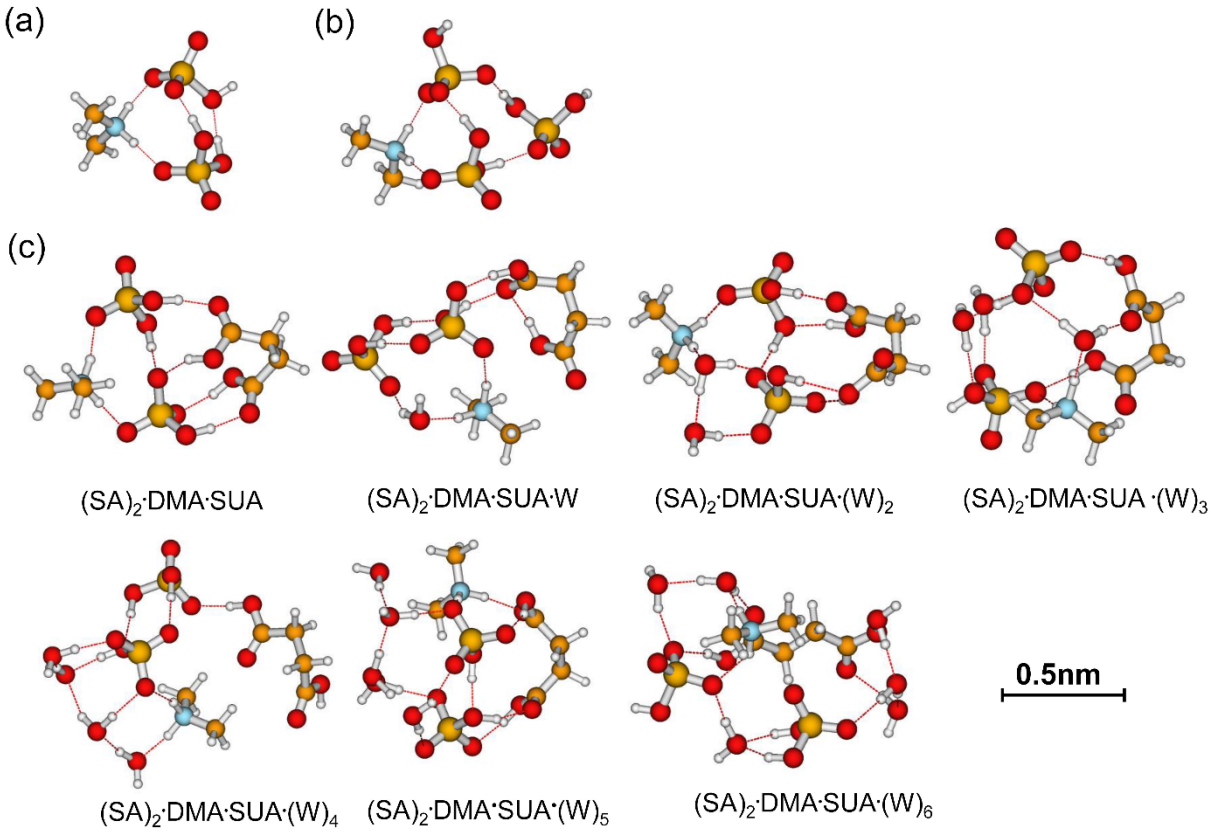


FIG. 6. Most stable configurations of (a) unhydrated $(SA)_2$•DMA, (b) $(SA)_2$•DMA, and (c) the hydrated $(SA)_2$•DMA•SUA clusters. The hydration is with 0-6 water molecules (W).

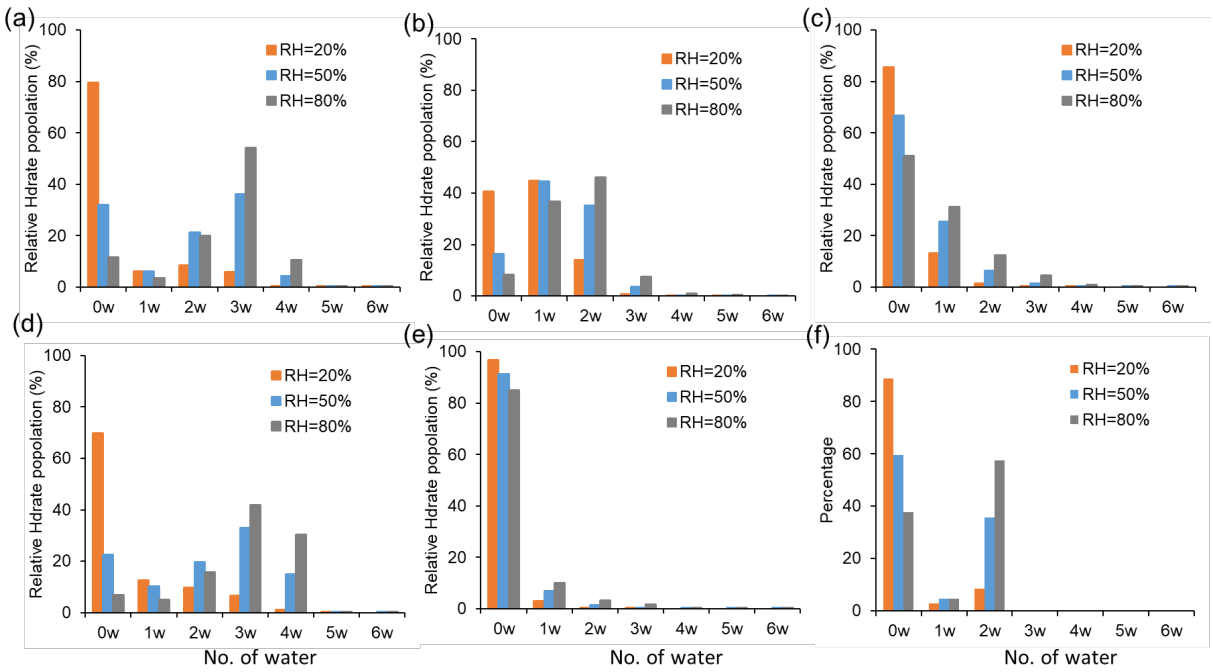


FIG. 7. Hydrate distributions of clusters under different RH levels (20%, 50% and 80%). (a), (b), and (c) are clusters for SA•AM, SA•DMA, and SA•DMA•AM, respectively. (d), (e) and (f) are clusters with one SUA addition on the basis of (a), (b) and (c) clusters. In all RH cases, T=298 K.

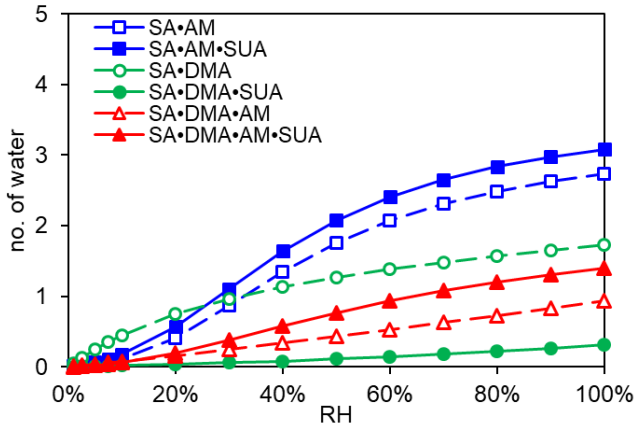


707

708 FIG. 8. Average hydration numbers per cluster for various SA•base clusters at 298.15 K.

709

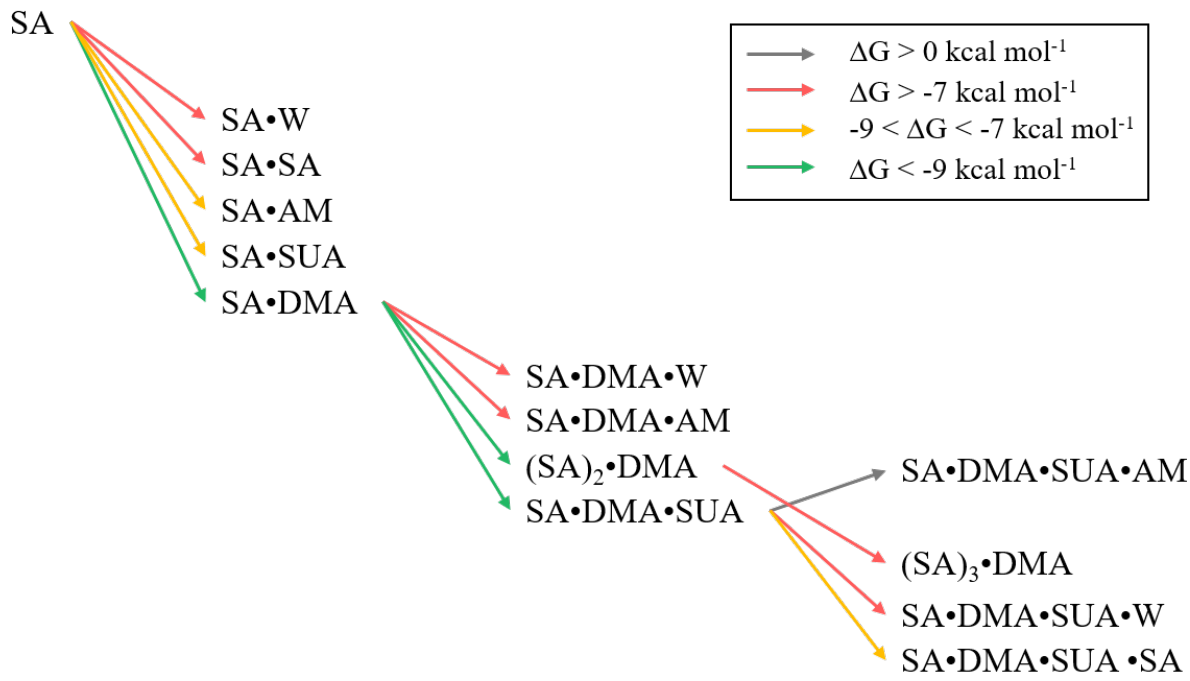


710

711 Fig. 9. Possible pathways for cluster formation based on free energies of formation.

712

713

714

715

716 Table 1. Theoretical and experimental values of the free energy change for several basic

717 reactions in kcal $mol^{-1}$.

| Reactions | This study | | refs |
|---|---|---|---|
| | PW91PW91/6-311++G(2df,2pd) | M06-2X/6-311++G(3df,3pd) | |
| SA+AM →SA•AM | -7.65 | -8.00 | -8.5[a,*], -7.77[b], -6.64[c], -7.84[d] |
| SA+DMA→SA•DMA | -11.13 | -11.24 | 13.66[c], 11.38[e] |
| SA•AM+W→SA•AM•W | -1.48 | -0.07 | -1.41[b], -1.67[f] |
| SA•DMA+W→SA•DMA•W | -3.06 | -3.63 | -3.67[e], -2.89[f] |
| SA•AM+SUA→SA•AM•SUA | -6.20 | -7.29 | - |
| SA•DMA+SUA →SA•DMA•SUA | -9.86 | -11.46 | - |

718 [a] From Hanson and Eisele (2002)

719 [b] From Nadykto and Yu (2007)

720 [c] From Kurtén et al. (2008)

721 [d] From Elm et al. (2012)

722 [e] From Nadykto et al. (2011)

723 [f] From Henschel et al. (2014)

724 [*] corresponds to experimental results.

725

726 Table 2. Calculated binding energy Δ*E*(ZPE), enthalpy Δ*H*, and Gibbs free energy Δ*G* (at

727 *T*=298.15 K and *p*=1 atm) at the PW91PW91/6-311++G(2d, 2p) level of theory for the hydrated

728 clusters. Energies are in kcal $mol^{-1}$.

| Reactions | *ΔE(ZPE)* | *ΔH* | *ΔG* |
|---|---|---|---|
| SA+AM → SA•AM | -15.95 | -16.51 | -7.65 |
| SA+AM+W → SA•AM•W | -26.40 | -28.02 | -9.13 |
| SA+AM+2W → SA•AM•$(W)_2$ | -39.14 | -41.58 | -12.33 |
| SA+AM+3W → SA•AM•$(W)_3$ | -49.96 | -52.98 | -15.11 |
| SA+AM+4W → SA•AM•$(W)_4$ | -59.63 | -63.30 | -16.32 |
| SA+AM+5W → SA•AM•$(W)_5$ | -69.20 | -73.58 | -16.26 |
| SA+AM+6W → SA•AM•$(W)_6$ | -78.71 | -83.37 | -18.64 |
| | | | |
| SA+DMA → SA•DMA | -21.16 | -21.11 | -11.13 |
| SA+DMA+W →SA• DMA•W | -33.46 | -34.13 | -14.19 |
| SA+DMA+2W → SA•DMA•$(W)_2$ | -45.02 | -46.60 | -16.51 |
| SA+DMA+3W → SA•DMA•$(W)_3$ | -54.37 | -56.57 | -17.62 |
| SA+DMA+4W → SA•DMA•$(W)_4$ | -62.47 | -65.25 | -18.56 |
| SA+DMA+5W → SA•DMA•$(W)_5$ | -75.68 | -79.92 | -20.31 |
| SA+DMA+6W → SA•DMA•$(W)_6$ | -84.43 | -89.24 | -20.16 |
| | | | |
| SA+SUA+AM → SA•SUA•AM | -34.19 | -34.69 | -13.85 |
| SA+SUA+AM+W → SA•SUA•AM•W | -45.65 | -47.18 | -15.85 |
| SA+SUA+AM+2W → SA•SUA•AM•$(W)_2$ | -58.95 | -61.44 | -18.70 |
| SA+SUA+AM+3W → SA•SUA•AM•$(W)_3$ | -70.41 | -73.52 | -21.47 |
| SA+SUA+AM+4W → SA•SUA•AM•$(W)_4$ | -80.92 | -84.95 | -23.47 |
| SA+SUA+AM+5W → SA•SUA•AM•$(W)_5$ | -86.75 | -90.96 | -20.48 |
| SA+SUA+AM+6W → SA•SUA•AM•$(W)_6$ | -98.52 | -104.27 | -22.80 |
| | | | |
| SA+SUA+DMA → SA•SUA•DMA | -42.01 | -41.42 | -20.98 |
| SA+SUA+DMA+W → SA•SUA•DMA•W | -54.80 | -55.47 | -21.92 |
| SA+SUA+DMA+2W → SA•SUA•DMA•$(W)_2$ | -64.86 | -66.03 | -23.45 |
| SA+SUA+DMA+3W → SA•SUA•DMA•$(W)_3$ | -75.90 | -78.21 | -25.19 |
| SA+SUA+DMA+4W → SA•SUA•DMA•$(W)_4$ | -82.83 | -86.21 | -21.95 |
| SA+SUA+DMA+5W → SA•SUA•DMA•$(W)_5$ | -92.80 | -96.19 | -26.54 |
| SA+SUA+DMA+6W → SA•SUA•DMA•$(W)_6$ | -103.04 | -107.49 | -27.29 |
| | | | |
| 2SA+SUA+DMA → $(SA)_2$•SUA•DMA | -62.90 | -63.35 | -26.12 |
| 2SA+SUA+DMA+W → $(SA)_2$•SUA•DMA•W | -69.95 | -70.90 | -25.11 |
| 2SA+SUA+DMA+2W → $(SA)_2$•SUA•DMA•$(W)_2$ | -79.07 | -80.72 | -25.30 |
| 2SA+SUA+DMA+3W → $(SA)_2$•SUA•DMA•$(W)_3$ | -91.67 | -94.06 | -28.71 |
| 2SA+SUA+DMA+4W → $(SA)_2$•SUA•DMA•$(W)_4$ | -93.90 | -96.57 | -24.36 |
| 2SA+SUA+DMA+5W → $(SA)_2$•SUA•DMA•$(W)_5$ | -115.58 | -120.45 | -31.69 |

| | | | |
|---|---|---|---|
| $2SA+SUA+DMA+6W \rightarrow (SA)_2 \bullet SUA \bullet DMA \bullet (W)_6$ | -108.55 | -112.07 | -22.50 |
| | | | |
| $SA+DMA+AM \rightarrow SA \bullet DMA \bullet AM$ | -23.83 | -33.01 | -14.15 |
| $SA+DMA+AM+W \rightarrow SA \bullet DMA \bullet AM \bullet W$ | -44.15 | -45.58 | -16.05 |
| $SA+DMA+AM+2W \rightarrow SA \bullet DMA \bullet AM \bullet (W)_2$ | -54.34 | -56.54 | -17.69 |
| $SA+DMA+AM+3W \rightarrow SA \bullet DMA \bullet AM \bullet (W)_3$ | -66.01 | -69.12 | -19.27 |
| $SA+DMA+AM+4W \rightarrow SA \bullet DMA \bullet AM \bullet (W)_4$ | -75.88 | -79.62 | -20.44 |
| $SA+DMA+AM+5W \rightarrow SA \bullet DMA \bullet AM \bullet (W)_5$ | -83.63 | -87.99 | -19.74 |
| $SA+DMA+AM+6W \rightarrow SA \bullet DMA \bullet AM \bullet (W)_6$ | -97.07 | -102.91 | -22.48 |
| | | | |
| $SA+SUA+DMA+AM \rightarrow SA \bullet SUA \bullet DMA \bullet AM$ | -54.69 | -56.03 | -20.69 |
| $SA+SUA+DMA+AM+W \rightarrow SA \bullet SUA \bullet DMA \bullet AM \bullet W$ | -62.07 | -63.89 | -21.65 |
| $SA+SUA+DMA+AM+2W \rightarrow SA \bullet SUA \bullet DMA \bullet AM \bullet (W)_2$ | -77.31 | -80.08 | -25.32 |
| $SA+SUA+DMA+AM+3W \rightarrow SA \bullet SUA \bullet DMA \bullet AM \bullet (W)_3$ | -83.64 | -87.00 | -24.00 |
| $SA+SUA+DMA+AM+4W \rightarrow SA \bullet SUA \bullet DMA \bullet AM \bullet (W)_4$ | -92.14 | -95.95 | -24.48 |
| $SA+SUA+DMA+AM+5W \rightarrow SA \bullet SUA \bullet DMA \bullet AM \bullet (W)_5$ | -104.97 | -110.11 | -25.51 |
| $SA+SUA+DMA+AM+6W \rightarrow SA \bullet SUA \bullet DMA \bullet AM \bullet (W)_6$ | -115.86 | -121.79 | -28.66 |

729
730

731 Table 3. Typical ranges of gas-phase concentrations (molecules $cm^{-3}$) for sulfuric acid,

732 ammonium, dimethylamine, and succinic acid in the atmosphere.

| Precursors | Sulfuric acid [a] | Ammonium[b] | Dimethylamine[c] | Succinic acid[d] |
|---|---|---|---|---|
| number concentration | $1x10^5$~$1x10^7$ | $1x10^9$~$1x10^{11}$ | $1x10^7$~$1x10^9$ | $1x10^8$~$1x10^9$ |

733 [a] Weber et al. (1999), Nieminen et al. (2009), and Zhang et al. (2012).

734 [b] Seinfeld and Pandis (1998).

735 [c] Kurten et al. (2008).

736 [d] Ho et al. (2007).

737

738 Table 4. Number of Proton Transfers within hydrated Clusters (T = 298.15 K).

| Cluster | No. of water | | | | | | |
|---|---|---|---|---|---|---|---|
| | *0* | *1* | *2* | *3* | *4* | *5* | *6* |
| SA[a] | 0 | 0 | 0 | 1 | 1 | 1 | 1 |
| SA•AM | 0 | 1 | 1 | 1 | 1 | 1 | 1 |
| SA•AM•SUA | 1 | 1 | 1 | 1 | 1 | 1 | 1 |
| SA•DMA | 1 | 1 | 1 | 1 | 1 | 1 | 1 |
| SA•DMA•SUA | 1 | 1 | 1 | 1 | 1 | 1 | 1 |
| SA•DMA•AM | 1 | 1 | 1 | 1 | 1 | 1 | 2 |
| SA•DMA•AM•SUA | 2 | 2 | 2 | 2 | 2 | 2 | 2 |

739 [a] From Xu and Zhang (2013)

740

741 Table 5. Laplacian bond order (LBO) of the newly formed covalent bond (nitrogen-hydrogen
742 bond) between in the clusters (a.u.).

| Clusters | Bonds | No. of water | | | | | | |
|---|---|---|---|---|---|---|---|---|
| | | *0* | *1* | *2* | *3* | *4* | *5* | *6* |
| SA•AM | N1-H1 | - | 0.383 | 0.577 | 0.586 | 0.580 | 0.636 | 0.663 |
| SA•AM•SUA | N1-H1 | 0.464 | 0.575 | 0.586 | 0.621 | 0.609 | 0.663 | 0.607 |
| SA•DMA | N2-H2 | 0.542 | 0.503 | 0.571 | 0.571 | 0.577 | 0.579 | 0.610 |
| SA•DMA•SUA | N2-H2 | 0.551 | 0.548 | 0.598 | 0.613 | 0.583 | 0.613 | 0.581 |
| SA•DMA•AM | N1-H1 | - | - | - | - | - | - | 0.525 |
| | N2-H2 | 0.489 | 0.483 | 0.608 | 0.553 | 0.533 | 0.591 | 0.567 |
| SA•DMA•AM•SUA | N1-H1 | 0.420 | 0.521 | 0.483 | 0.321 | 0.607 | 0.591 | 0.677 |
| | N2-H2 | 0.498 | 0.411 | 0.518 | 0.611 | 0.501 | 0.564 | 0.568 |

743 Note: N1 is the nitrogen atom on the ammonia (AM) molecule; N2 is the nitrogen atom on the
744 dimethylamine (DMA) molecule; H1 is the hydrogen atom on one of the hydroxyl functions of sulfuric
745 acid (SA) molecule and bound to N1; H2 is the hydrogen atom on one of the hydroxyl functions of SA
746 (SA) molecule and bound to N2.

747

748 Table 6. Gibbs free energy (ΔG, kcal $mol^{-1}$), interaction energy (ΔH0, kcal $mol^{-1}$), and typical cluster concentration at equilibrium for
749 basic clustering reactions. The right-hand side of clustering reactions is the product clusters in equation (9), and the core clusters and
750 addition molecules in equation (9) are listed here as well.

| Cluster reactions | ΔG | ΔH0 | Cluster | | |
|---|---|---|---|---|---|
| | | | Core cluster | Molecule for addition | [Cluster] ($cm^{-3}$) |
| SA+SA ↔ $(SA)_2$ | -3.72 | -13.08 | SA | SA | $10^{-7}$~$10^{-3}$ |
| SA+SUA ↔ SA•SUA | -8.61 | -17.94 | SA | SUA | $10^{0}$~$10^{3}$ |
| SA+AM ↔ SA•AM | -6.36 | -14.38 | SA | AM | $10^{-1}$~$10^{-3}$ |
| SA+DMA ↔ SA•DMA | -11.41 | -18.38 | SA | DMA | $10^{1}$~$10^{5}$ |
| | | | | | |
| SA•SUA+SA ↔ $(SA)_2$•SUA | -1.02 | -11.04 | SA•SUA | SA | $10^{-14}$~$10^{-9}$ |
| SA•AM+SA ↔ $(SA)_2$•AM | -9.46 | -19.53 | SA•AM | SA | $10^{-9}$~$10^{-3}$ |
| SA•AM+SUA ↔ SA•AM•SUA | -6.20 | -16.01 | SA•AM | SUA | $10^{-8}$~$10^{-3}$ |
| SA•DMA+SA ↔ $(SA)_2$•DMA | -10.53 | -21.16 | SA•DMA | SA | $10^{-6}$~$10^{0}$ |
| SA•DMA+SUA ↔ SA•DMA•SUA | -9.86 | -19.07 | SA•DMA | SUA | $10^{-3}$~$10^{2}$ |
| | | | | | |
| $(SA)_2$•DMA+SA ↔ $(SA)_3$•DMA | -6.10 | -15.25 | $(SA)_2$•DMA | SA | $10^{-16}$~$10^{-8}$ |
| SA•DMA•SUA+SA ↔ $(SA)_2$•DMA•SUA | -5.13 | -19.07 | SA•DMA•SUA | SA | $10^{-14}$~$10^{-7}$ |

751

752 Table 7. Concentration Ratios between SUA•SA•X and $(SA)_2$•X Clusters, with X = W, AM, and

753 DMA.

| SUA/SA | X=(None) | X=W | X=AM | X=DMA |
|---|---|---|---|---|
| 0.1:1 | 3.80E+02 | 5.30E+01 | 4.11E-04 | 3.19E-02 |
| 1:1 | 3.80E+03 | 5.30E+02 | 4.11E-03 | 3.19E-01 |
| 10:1 | 3.80E+04 | 5.30E+03 | 4.11E-02 | 3.19E+00 |
| 100:1 | 3.80E+05 | 5.30E+04 | 4.11E-01 | 3.19E+01 |

754